CARBON 52 (2013) 528–534

Available at www.sciencedirect.com

SciVerse ScienceDirect

journal homepage: www.elsevier.com/locate/carbon

Rapid and non-destructive identification of graphene oxide thickness using white light contrast spectroscopy

Huanping Yang [a], *Hailong Hu* [a], *Yingying Wang* [b], *Ting Yu* [a,c,d,*]

[a] *Division of Physics and Applied Physics, School of Physical and Mathematical Sciences, Nanyang Technological University, 637371 Singapore, Singapore*

[b] *Harbin Institute of Technology at Weihai, 264209 Weihai, China*

[c] *Department of Physics, Faculty of Science, National University of Singapore, 117542 Singapore, Singapore*

[d] *Graphene Research Centre, National University of Singapore, 2 Science Drive 3, Singapore 117542, Singapore*

ARTICLE INFO

Article history:
Received 11 July 2012
Accepted 4 October 2012
Available online 12 October 2012

ABSTRACT

By white light contrast spectroscopy, we have successfully identified number of graphene oxide (GO) layers (⩽10 layers) and obtained a new refractive index of GO sheets (⩽10 layers) of n_{GO} = 1.2–0.24i. For few layers (⩽10 layers) GO sheets, both the contrast at ~580 nm wavelength and the Raman intensity of G band linearly increase with the increase of the layer numbers. However, due to the laser induced heating effects and the requirement of a reference Raman spectrum in Raman spectroscopy measurements, contrast spectroscopy is non-destructive and more efficient. Simulations based on the Fresnel's equations agree well with evolution of the contrast and G band intensity as a function of number of layers. The precise refractive index of GO obtained in this work can be widely used in further study of GO. Therefore, our experimental contrast values can be directly used as a standard to identify the thickness of GO on Si substrate with 300 nm SiO_2 capping layer, which paves a novelty way towards future fundamental research and applications of graphene-based materials.

1. Introduction

Graphene oxide (GO) sheets, free-standing two-dimensional compounds with a variable ratio of carbon, oxygen and hydrogen, have attracted significant attention because GO sheets can be used for highly sensitive biosensing [4], biocompatible drug delivery [5], energy [6,7] and high-capacity hydrogen storage [8,9]. The electrical, mechanical, thermal and optical properties of GO are strongly dependent on the chemical and atomic structure [10–14], which can cover a broad scope via chemical approaches. However, the determination of number of GO layers remains to challenge to fully understand and further develop potential applications for GO sheets. A fast and accurate method for identifying the thickness of GO sheets will intensify the study and exploration of GO sheets. In the past few years, many methods [1,2,15–18] have been developed to identify the number of graphene layers, but only the optical methods are non-destructive and facile, such as Raman spectroscopy [15,19–23], contrast spectroscopy [24], Rayleigh spectroscopy [25] and optical microscopy [26–28]. Due to the weak optical absorbance that originates from both the large optical gap caused by sp^3 hybridization of the functional groups and the adsorbed water on GO sheets, the identification of the thickness of GO sheets has been only rarely studied. Compare to graphene, GO sheets have a paler color and weaker optical absorbance. Moreover, GO sheets can be easily reduced or damaged by the laser or heating. Some optical microscopy, which is used

* *Corresponding author at:* Division of Physics and Applied Physics, School of Physical and Mathematical Sciences, Nanyang Technological University, 637371 Singapore, Singapore.
E-mail address: yuting@ntu.edu.sg (T. Yu).

0008-6223/$ - see front matter
http://dx.doi.org/10.1016/j.carbon.2012.10.005

to characterize graphene [26–28], is not an ideal method to directly and accurately identify the thickness of GO sheets. Up to now, only a few papers reported the visualization of GO sheets by fluorescence quenching microscopy (FQM) [29–32], which was not capable of identifying the number of GO layers. For the accurate identification GO thickness, a more direct and efficient method is desirable. Jung et al. [3] utilized a laser source with three different wavelengths to obtain a high-contrast optical image of GO sheets. However, the three individual contrast values could not provide a complete response of GO layers over the entire optical region, which may limit the general adaptation of this method due to the strict requirements of laser sources. In addition, in contrast to graphene or reduced GO sheets, GO is very sensitive to laser irradiation and easily reduced by laser induced heating [33,34]. Therefore, low-power-based optical contrast spectroscopy, with its advantages of rapid and non-destructive, is a unique technique for identifying GO sheets. In this work, a white light source is used to identify the number of GO layers. This technique enables a contrast spectrum to be acquired ranging from 420 to 800 nm. In comparison, Raman spectroscopy is employed to determine the number of GO layers. While accounting for the laser heating and the requirement of a reference spectrum for the Raman spectroscopy, the contrast spectra and images can accurately and directly determine the thickness of GO sheets. To further understand the contrast spectra of GO sheets, Fresnel's equations are used to simulate the contrast of GO sheets [24]. The simulation results were well-matched with the experimental data within the range from 520 to 800 nm. The experimental data can be used as a criterion to determine the number of GO layers accurately and directly.

2. Experimental

2.1. Chemicals

Commercial expanded graphite, 98% H_2SO_4, 30% H_2O_2, 85% H_3PO_4 and $KMnO_4$ from Sigma–Aldrich were used without further purification. Distilled water was used in all the processes of aqueous solution preparation and washing.

2.2. Synthesis of GO

Commercial expanded graphite (CEG) was used to synthesize GO by a modified Hummers method [35–37]. In a different manner from our previous work [38], 3 g of CEG was added into a 9:1 mixture of concentrated H_2SO_4/H_3PO_4 (360:40 mL) in a flask, which was immersed in an ice bath. Afterwards, 15 g of $KMnO_4$ was slowly added to the solution. Meanwhile, the temperature of the mixed solution was maintained below 20 °C for 2 h to avoid overheating and explosion. The mixture was stirred for five days. Subsequently, 10 mL of 30% H_2O_2 was added to the solution to completely react with the remaining $KMnO_4$, resulting in a bright yellow solution. Finally, the mixture was washed with H_2O until the pH of the solution was approximately 5. GO powder was obtained after freeze drying the suspension.

2.3. Preparation of thin-film GO

Si wafer with a 300 nm SiO_2 (SiO_2/Si) capping layer was used as a substrate for preparing GO films. The SiO_2/Si substrates were cleaned in piranha solution [11] (a 3:1 mixture of concentrated 98% H_2SO_4 and 30% H_2O_2) at 100 °C for 1 h. The surfaces of the SiO_2/Si substrates became hydrophilic after the piranha treatment. The GO films were deposited onto the SiO_2/Si substrates by the dip-coating method.

2.4. Contrast and Raman measurement

Both contrast and Raman spectra were measured on a WITEC CRM200 Raman system with a 100× objective. For contrast measurement, we used a normal white light (tungsten halogen lamp, excitation range from 400 to 800 nm, across a 1 mm slit) as the source to emit the incident light. The reflected light was collected via backscattering configuration (with a 100 μm pinhole) and directed to a 150 lines/mm grating and detected with a TE-cooled charge-coupled-device (CCD). The reflection spectra obtained from GO were compared with that from a background spectrum of SiO_2/Si to generate the contrast spectra. For Raman measurement, the excitation source is 532 nm with a laser power 0.1 mW. A short integration time 3 s was used in this measurement in order to reduce the effect of laser-induced heating as much as possible. The contrast and Raman images were obtained by scanning the sample on a piezostage under illumination of white light and laser, respectively. The ScanCtrl Spectroscopy Plus software (WITec GmbH, Germany) controlled the stage movement and recorded the data point by point. WITec Project software is used to perform the analysis of the spectra and mapping images.

3. Results and discussions

Fig. 1a presents an optical image of GO sheets on a SiO_2/Si substrate. The GO sheets show five areas of different contrast, which are likely due to five different thicknesses. The thicknesses of the GO sheets are further investigated by tapping mode AFM and the image is shown in Fig. 1b. From the inset of the height profiles in Fig. 1b, the thickness of single-layer GO sheet is observed to be approximately 1 nm (the inset of the height profile with white color) [10,39–41]. As the number of layers increases, the thickness linearly increases. For example, 2.1, 3.2, 4.2 and 5.3 nm correspond to two, three, four and five layers, respectively (the inset of the height profile with green color). Fig. 1c displays the typical Raman spectra of a GO sheet with a single-layer to five-layer sample, which were measured under the same conditions. The two main peaks observed at 1342 and 1589 cm^{-1} are the D and G band, respectively [33]. As shown in the inset image in Fig. 1c, the intensity of the G band increases linearly as the number of GO layers increases, which is similar to observations reported in previous work [34]. Fig. 1d shows the typical Raman mapping of a GO sheet with a single-layer to five-layer sample plotted against the G band intensity of the GO sheet. It clearly presents five different intensities.

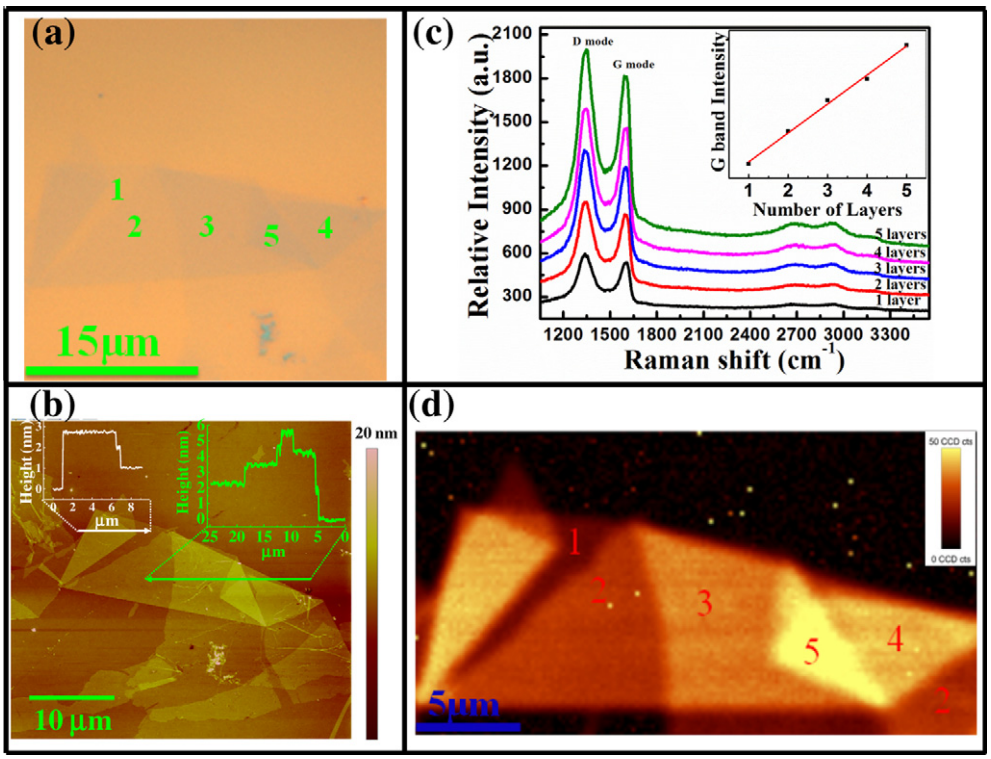

Fig. 1 – (a) and (b) Optical and cross-sectional AFM images of GO sheets with 1–5 layers, respectively. The inset curves in (b) represent the z-profiles. (c) The Raman spectra as a function of the number of layers, which shows a linear relationship between the G band intensity and the number of GO layers. (d)The Raman image plotted against the G band intensity of the GO sheet.

To further extend the scope of the above mentioned G-intensity method, a thicker GO sheet (⩾5 layers) was studied. The thicknesses of the GO layers were characterized by AFM (Fig. 2a). Fig. 2b shows the optical image of the homologous GO sheets, which are labeled by the number of the layers according to the corresponding z-profiles from the AFM image. Similar to the 1–5 layered GO sheets, the Raman intensity of G band was observed to linearly increase as the number of GO sheets increased to 10 layers, and similar observations were made for few-layer graphene [42]. For more than 10 layers, the intensity of the G band slightly increases (10–27 layers), and then decreases as the number of GO layers increases. Although the linear relationship between the G band intensity and GO sheet thickness (⩽10 layers) exists, the precise identify number of layers of the GO sheet cannot be identified, because the absolute Raman band intensity can be affected by many factors. To use this method, a pre-determined single layer GO sheet is required as a reference. In addition to the lack of a reference spectrum, laser-induced heating is another major impediment, which will be discussed later.

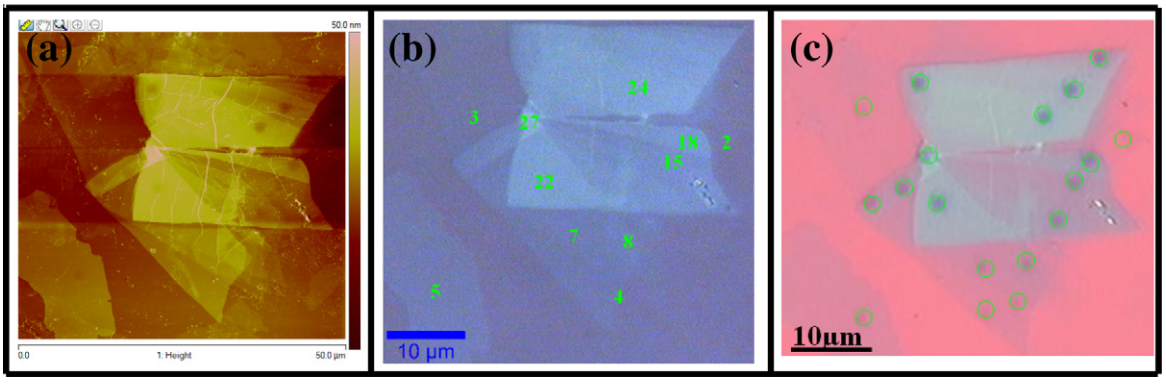

Fig. 2 – (a) AFM image of GO sheets with various thicknesses. (b) The corresponding optical image of the GO, which is marked by the number of the layers identified by AFM. (c) The optical image of the GO sheets after Raman measurements. The green circles show the area reduced by the laser. (For interpretation of the references to colour in this figure legend, the reader is referred to the web version of this article.)

During the Raman measurements, the areas irradiated by the laser beam were observed to darken in the optical image as shown in Fig. 2c, and are marked by green circles.

To investigate the effects of laser-induced heating on GO sheets, two-step Raman mapping was performed. Firstly, a 4×4 μm square region was scanned at a laser power of 0.1 mW, and the integration time for each spectrum was 0.5 s. These conditions were used because the laser-induced heating effects were minimal and an acceptable Raman signal to noise ratio was achieved. Subsequently, a larger area, which included the square area previously mapped, was mapped under the same condition as in the first step (Fig. 3a). Although a very low laser power and short integration time were used for the acquisition of Raman measurements, reduction [34] of the GO sheets by the laser irradiation was unavoidable. The dark area highlighted by the dash line in Fig. 3a provides evidence for this effect [33,34] As shown in Fig. 3b, the decrease in the Raman intensity before and after Raman mapping is obvious, which indicates that laser irradiation greatly influences the GO sheets. The decrease of intensity of the Raman modes is due to the partial removal of functional groups from the GO with the laser irradiation during the Raman measurements. These effects prohibit the use of Raman spectroscopy as a reliable method to identify the thickness of GO sheets.

Because the Raman measurements always reduce the GO sheets due to laser-induced heating, contrast spectroscopy and mapping under white light illumination were exploited to determine the thickness of GO sheets.

The origin of the contrast can be explained by Fresnel's equations. Consider the incident light from air ($n_0 = 1$) onto a GO, SiO_2, and Si trilayer system. The reflection amplitude from the air/GO/SiO_2/Si system, r'_g, can be calculated by Fresnel equation,

$$r'_g = \frac{r_{01} + r' \cdot e^{-2i\cdot\phi_1}}{1 + r_{01}\cdot r' \cdot e^{-2i\cdot\phi_1}} \quad (1)$$

$$r' = \frac{r_{12} + r_{23} \cdot e^{-2i\cdot\phi_1}}{1 + r_{12}\cdot r_{23} \cdot e^{-2i\cdot\phi_2}} \quad (2)$$

Here, r' is the reflection coefficient at the GO/(SiO_2 on Si) interface. $r_{01} = \frac{n_0-n_1}{n_0+n_1}$ is the reflection coefficient at the air/GO interface. $r_{12} = \frac{n_1-n_2}{n_1+n_2}$ is the reflection coefficient at the GO/SiO_2 interface. $r_{23} = \frac{n_2-n_3}{n_2+n_3}$ is the reflection coefficient at the SiO_2/Si interface) $n_1\cdot(n_2,\cdot n_3)$ is the refractive index of GO (SiO_2, Si). $\phi_{1,2} = \frac{2\pi\cdot n_{1,2}\cdot d_{1,2}}{\lambda}$ is the phase difference when light passes through GO or SiO_2 layer. The reflection spectrum from the air/GO/SiO_2/Si system, $R(\lambda)$ can be calculated by

$$R(\lambda) = |r'_g|^2 \quad (3)$$

The reflection spectrum from air/SiO_2/Si system $R_0(\lambda)$ is calculated following the same method. Finally, the contrast spectrum $C(\lambda)$ of GO can be obtained by

$$C(\lambda) = \frac{R_0(\lambda) - R(\lambda)}{R_0(\lambda)} \quad (4)$$

Fig. 4 shows the contrast spectra for GO sheets of various thicknesses on a SiO_2/Si substrate. A peak at approximately 588 nm (in the visible range) was observed in the contrast spectrum of a single-layered GO sheet, which almost maintains a constant value as the number of layers (within 10 layers) increased. The contrast value for the single-layer GO sheet was approximately 0.035 ± 0.005 and increased as the number of layers increased. For thicker GO sheets (>10 layers), the contrast peaks show a red shift. The shift is caused by different phase differences, which are determined by the path difference of two neighboring light beams that have interference ($\beta = 2\Pi n(d/\lambda)$) [24]. Where n is the refractive index of GO and d is the thickness of GO, which can be estimated as $d = N\Delta d$ ($\Delta d = 1$ nm). Fresnel's equations are used to explain the evolution of the contrast values. The simulation results are discussed below.

Regarding the incident light into the trilayered system (air to the GO sheet to the SiO_2/Si), the contrast spectrum was calculated. The thickness of the SiO_2 was 300 nm and the Si substrate was assumed to be semi-infinite. The thickness of GO sheets was estimated to be $N^*\Delta d$, where $\Delta d = 1$ nm, is the average thickness of a single layer of GO and N is the number of layers. The refractive index of the materials are $n_{air} \approx 1$, $n_{SiO2} = 1.46$ and $n_{Si} = 4.15–0.044i$ in the white light region ranging from 400–800 nm, respectively. Firstly, the refraction index $n_{GO} = 1.7–0.2i$ (blue line in Fig. 5) was used as suggested previously [43]. The results of the calculations showed large deviations from experimental data. Modification of the refractive

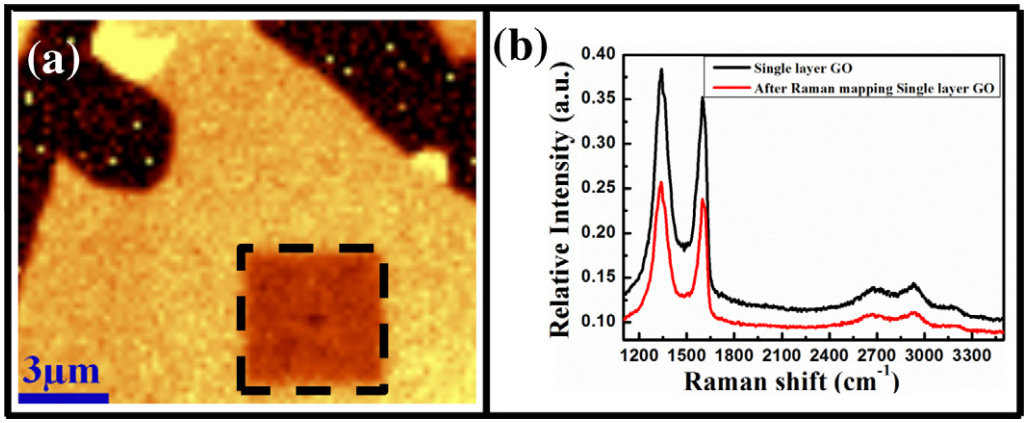

Fig. 3 – (a) The Raman image plotted by the intensity of the G band of the GO sheets. The area marked by the black dashed line was scanned twice. (b) Raman spectra of the single layer GO sheet (black curve) and laser-reduced GO sheet (red curve). (For interpretation of the references to colour in this figure legend, the reader is referred to the web version of this article.)

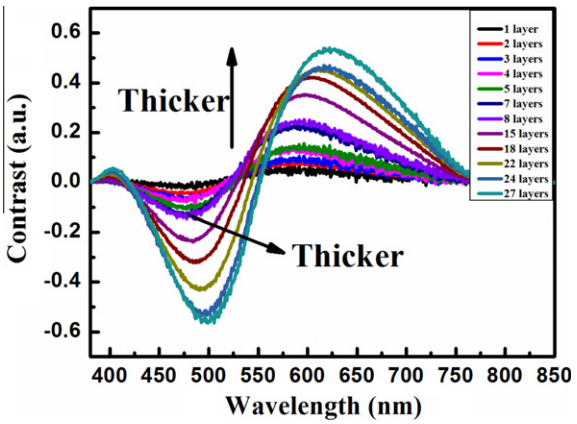

Fig. 4 – The contrast spectra of GO sheets with different thicknesses.

index was performed to have a better fit with the experiment results, The optimized refractive index of a single-layer of a GO sheet was determined to be n_{GO} = 1.2–0.24i (red line in Fig. 5). This new refractive index was also used to fit the spectra of few-layered GO sheet. The close agreement between the simulated and experimental results supports the accuracy of the refractive index (Fig. 6).

A disagreement between the simulated and experimental results can be observed in the range of 420–520 nm. The reason for the deviation is not clear. One possibility is that when the contrast of the GO was calculated, the influence of the functional groups and water on the GO sheets was not considered. The contrast of the GO sheet may be influenced. Further investigation is required.

For the identification of the thickness of a GO sheet, the accurate and effective way is to use the contrast spectra in the range 520–800 nm.

Because the Raman band intensities of multiple layer structures are sensitive to the refractive index, the new refractive index (n_{GO} = 1.2–0.24i) was used to fit the intensity

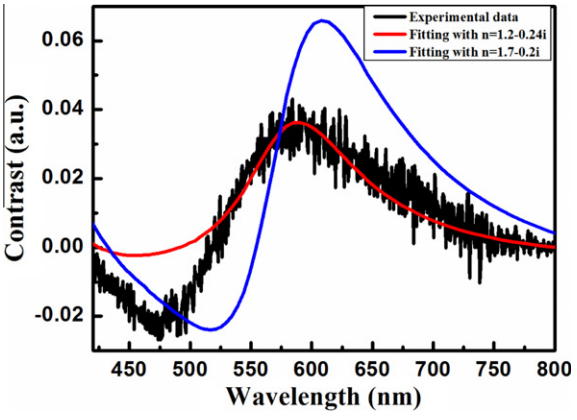

Fig. 5 – Typical contrast spectra of a single-layered GO sheet obtained from experiment (black line), the calculation using n = 1.2–0.24i (red line) and n = 1.7–0.2i (blue line). (For interpretation of the references to colour in this figure legend, the reader is referred to the web version of this article.)

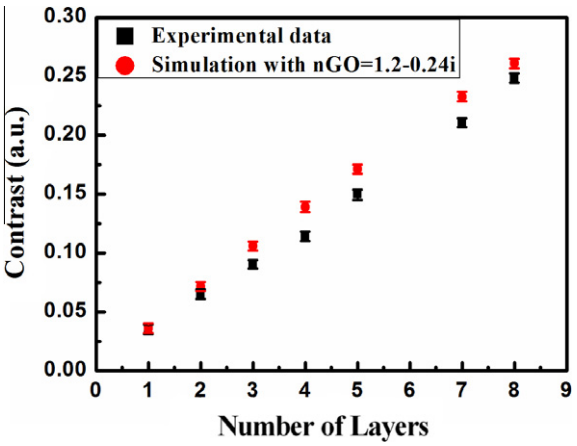

Fig. 6 – The contrast values of experimental data (black square) and the simulated results using n = 1.2–0.24i (red sphere) for 1–8 layers of GO sheets. (For interpretation of the references to colour in this figure legend, the reader is referred to the web version of this article.)

of the Raman G band based on Fresnel's equations (shown in Fig. 7). Good agreement between the experimental data and the simulation curve can been clearly observed in Fig. 7. The significant improvement over previously reported values indicates that the refractive index of GO determined in this work could be widely used in the future study of GO sheets. For a GO sheet of unknown thickness, contrast spectroscopy can directly determine the thickness by comparing the contrast value with the standard values shown in Fig. 6. Alternatively, the thickness can also be obtained from our empirical equation.

$$C = 0.01393 + 0.02264N + 0.000818007N^2 \quad (5)$$

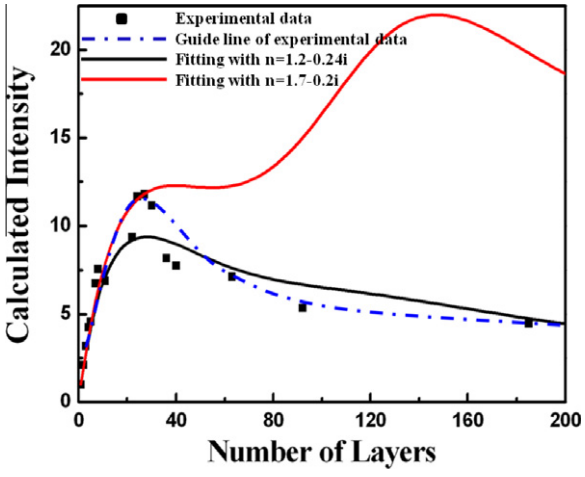

Fig. 7 – The experimental (the blue dash-dot line curve is a guide for the eye) and calculated results of the G band intensity as a function of number of layers using n = 1.2–0.24i (black line) and n = 1.7–0.2i (red line). (For interpretation of the references to colour in this figure legend, the reader is referred to the web version of this article.)

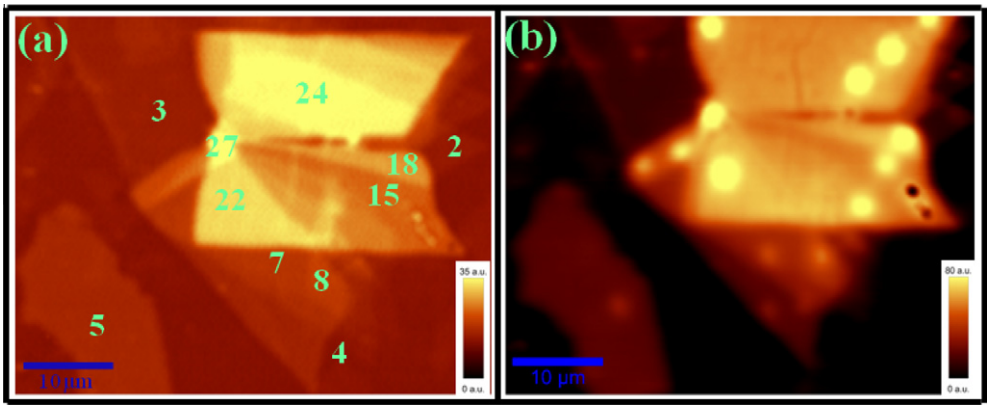

Fig. 8 – (a) The contrast image of GO sheets with a varied number of layers before laser exposure. (b) The contrast image of the sample after the collection of a single Raman spectrum.

where N ($\leqslant$10) is the number of layers of GO. Eq. (5) was obtained by fitting the experimental data.

To further confirm the effectiveness of the contrast spectra for the determination of the thickness of GO sheets, contrast mapping was performed. Fig. 8a shows the contrast image of the same sample shown in Fig. 2. It is worth noting that the contrast image provides a better perspective view of the sample. As was observed in the Raman image plotted by the intensity of the G band, thicker GO sheets resulted in higher contrast. Fig. 8b shows the contrast image of the same sample collected after the single Raman spectrum measurement with a laser power of 0.1 mW and integration time of 3 s. The obvious change in the contrast of the GO before and after laser irradiation indicates that Raman spectroscopy is inappropriate for thickness determination. Moreover, a high quality contrast image can be acquired more quickly than a Raman image, which results in a high-throughput method relative to the Raman method. Contrast spectroscopy and mapping can enable a nondestructive and more efficient way to characterize the thickness of GO sheets to be achieved without changing the sample.

4. Conclusion

In conclusion, the facile and effective determination of the number of GO layers was demonstrated using contrast spectroscopy. A new refractive index for GO sheets ($\leqslant$10 layer) was obtained n_{GO} = 1.2–0.24i. The agreement between the simulated results and experimental data, for both the contrast and G band intensities suggests that this new refractive index can be used in further GO studies. Contrast mapping further demonstrated that this method is a convenient and powerful probe for the quick visualization of GO sheets of different thicknesses. As additional properties are discovered and new applications are proposed for single- and few-layered GO sheets, contrast spectroscopy (an accurate, easy-to-achieve and fast method to determine the thickness of GO layers less than 10 layers thick) will become very useful for future fundamental and practical studies.

Acknowledgement

This work is supported by the Singapore National Research Foundation under NRF RF Award No. NRF RF2010-07 and MOE Tier 2 MOE 2009-T2-1-037.

REFERENCES

[1] Novoselov KS, Geim AK, Morozov SV, Jiang D, Zhang Y, Dubonos SV, et al. Electric field effect in atomically thin carbon films. Science 2004;306(5696):666–9.
[2] Novoselov KS, Jiang D, Schedin F, Booth TJ, Khotkevich VV, Morozov SV, et al. Two-dimensional atomic crystals. Proc Natl Acad Sci USA 2005;102(30):10451–3.
[3] Jung I, Pelton M, Piner R, Dikin DA, Stankovich S, Watcharotone S, et al. Simple approach for high-contrast optical imaging and characterization of graphene-based sheets. Nano Lett 2007;7(12):3569–75.
[4] Lu CH, Yang HH, Zhu CL, Chen X, Chen GN. A graphene platform for sensing biomolecules. Angew Chem Int Ed 2009;48(26):4785–7.
[5] Liu Z, Robinson JT, Sun XM, Dai HJ. PEGylated nanographene oxide for delivery of water-insoluble cancer drugs. J Am Chem Soc 2008;130(33). 10876–+.
[6] Zhou WW, Zhu JX, Cheng CW, Liu JP, Yang HP, Cong CX, et al. A general strategy toward graphene@metal oxide core–shell nanostructures for high-performance lithium storagec. Energy Environ Sci 2012:4954–61.
[7] Zhou WW, Liu JP, Chen T, Tan KS, Jia XT, Luo ZQ, et al. Fabrication of Co(3)O(4)-reduced graphene oxide scrolls for high-performance supercapacitor electrodes. Phys Chem Chem Phys 2011;13(32):14462–5.
[8] Wang L, Lee K, Sun YY, Lucking M, Chen ZF, Zhao JJ, et al. Graphene oxide as an ideal substrate for hydrogen storage. ACS Nano 2009;3(10):2995–3000.
[9] Hu ZL, Aizawa M, Wang ZM, Yoshizawa N, Hatori H. Synthesis and characteristics of graphene oxide-derived carbon nanosheet-Pd nanosized particle composites. Langmuir 2010;26(9):6681–8.
[10] Jung I, Dikin DA, Piner RD, Ruoff RS. Tunable electrical conductivity of individual graphene oxide sheets reduced at "low" temperatures. Nano Lett 2008;8(12):4283–7.
[11] Su CY, Xu YP, Zhang WJ, Zhao JW, Tang XH, Tsai CH, et al. Electrical and spectroscopic characterizations of ultra-large

reduced graphene oxide monolayers. Chem Mater 2009;21(23):5674–80.
[12] Zhan D, Ni ZH, Chen W, Sun L, Luo ZQ, Lai LF, et al. Electronic structure of graphite oxide and thermally reduced graphite oxide. Carbon 2011;49(4):1362–6.
[13] Mattevi C, Eda G, Agnoli S, Miller S, Mkhoyan KA, Celik O, et al. Evolution of electrical, chemical, and structural properties of transparent and conducting chemically derived graphene thin films. Adv Funct Mater 2009;19(16):2577–83.
[14] Becerril HA, Mao J, Liu Z, Stoltenberg RM, Bao Z, Chen Y. Evaluation of solution-processed reduced graphene oxide films as transparent conductors. ACS Nano 2008;2(3):463–70.
[15] Ferrari AC, Meyer JC, Scardaci V, Casiraghi C, Lazzeri M, Mauri F, et al. Raman spectrum of graphene and graphene layers. Phys Rev Lett 2006;97(18):187401-1–4.
[16] Pisana S, Lazzeri M, Casiraghi C, Novoselov KS, Geim AK, Ferrari AC, et al. Breakdown of the adiabatic Born-Oppenheimer approximation in graphene. Nat Mater 2007;6(3):198–201.
[17] Warner JH. The influence of the number of graphene layers on the atomic resolution images obtained from aberration-corrected high resolution transmission electron microscopy. Nanotechnology 2010;21(25):255707-1–5.
[18] Xu MS, Fujita D, Gao JH, Hanagata N. Auger electron spectroscopy: a rational method for determining thickness of graphene films. ACS Nano 2010;4(5):2937–45.
[19] Graf D, Molitor F, Ensslin K, Stampfer C, Jungen A, Hierold C, et al. Spatially resolved raman spectroscopy of single- and few-layer graphene. Nano Lett 2007;7(2):238–42.
[20] Gupta A, Chen G, Joshi P, Tadigadapa S, Eklund PC. Raman scattering from high-frequency phonons in supported *n*-graphene layer films. Nano Lett 2006;6(12):2667–73.
[21] Malard LM, Pimenta MA, Dresselhaus G, Dresselhaus MS. Raman spectroscopy in graphene. Phys Rep Rev Sec Phys Lett 2009;473(5–6):51–87.
[22] Caridad JM, Rossella F, Bellani V, Grandi MS, Diez E. Automated detection and characterization of graphene and few-layer graphite via Raman spectroscopy. J Raman Spectrosc 2011;42(3):286–93.
[23] Cong CX, Yu T, Saito R, Dresselhaus GF, Dresselhaus MS. Second-order overtone and combination Raman modes of graphene layers in the range of 1690–2150 cm(-1). ACS Nano 2011;5(3):1600–5.
[24] Ni ZH, Wang HM, Kasim J, Fan HM, Yu T, Wu YH, et al. Graphene thickness determination using reflection and contrast spectroscopy. Nano Lett 2007;7(9):2758–63.
[25] Casiraghi C, Hartschuh A, Lidorikis E, Qian H, Harutyunyan H, Gokus T, et al. Rayleigh imaging of graphene and graphene layers. Nano Lett 2007;7(9):2711–7.
[26] Teo GQ, Wang HM, Wu YH, Guo ZB, Zhang J, Ni ZH, et al. Visibility study of graphene multilayer structures. J Appl Phys 2008;103(12):124302-1–6.
[27] Chen YF, Liu D, Wang ZG, Li PJ, Hao X, Cheng K, et al. Rapid determination of the thickness of graphene using the ratio of color difference. J Phys Chem C 2011;115(14):6690–3.
[28] Roddaro S, Pingue P, Piazza V, Pellegrini V, Beltram F. The optical visibility of graphene: interference colors of ultrathin graphite on SiO(2). Nano Lett 2007;7(9):2707–10.
[29] Kim J, Cote LJ, Kim F, Huang JX. Visualizing graphene based sheets by fluorescence quenching microscopy. J Am Chem Soc 2010;132(1):260–7.
[30] Loh KP, Bao QL, Eda G, Chhowalla M. Graphene oxide as a chemically tunable platform for optical applications. Nat Chem 2010;2(12):1015–24.
[31] Kim J, Kim F, Huang JX. Seeing graphene-based sheets. Mater Today 2010;13(3):28–38.
[32] Treossi E, Melucci M, Liscio A, Gazzano M, Samori P, Palermo V. High-contrast visualization of graphene oxide on dye-sensitized glass, quartz, and silicon by fluorescence quenching. J Am Chem Soc 2009;131(43). 15576–+.
[33] Sokolov DA, Shepperd KR, Orlando TM. Formation of graphene features from direct laser-induced reduction of graphite oxide. J Phys Chem Lett 2010;1(18):2633–6.
[34] Zhou Y, Bao QL, Varghese B, Tang LAL, Tan CK, Sow CH, et al. Microstructuring of graphene oxide nanosheets using direct laser writing. Adv Mater 2010;22(1). 67–+.
[35] Hernandez Y, Nicolosi V, Lotya M, Blighe FM, Sun ZY, De S, et al. High-yield production of graphene by liquid-phase exfoliation of graphite. Nat Nanotechnol 2008;3(9):563–8.
[36] Hummers WS, Offeman RE. Preparation of graphitic oxide. J Am Chem Soc 1958;80(6):1339.
[37] Xu YX, Bai H, Lu GW, Li C, Shi GQ. Flexible graphene films via the filtration of water-soluble noncovalent functionalized graphene sheets. J Am Chem Soc 2008;130(18). 5856–+.
[38] Yang HP, Jiang J, Zhou WW, Lai LL, Xi LF, Lam YM, et al. Influences of graphene oxide support on the electrochemical performances of graphene oxide-MnO_2 nanocomposites. Nanoscale Research Letter 2011;6:5311–8.
[39] Eda G, Chhowalla M. Chemically derived graphene oxide: towards large-area thin-film electronics and optoelectronics. Adv Mater 2010;22(22):2392–415.
[40] Compton OC, Nguyen ST. Graphene oxide, highly reduced graphene oxide, and graphene: versatile building blocks for carbon-based materials. Small 2010;6(6):711–23.
[41] Acik M, Mattevi C, Gong C, Lee G, Cho K, Chhowalla M, et al. The role of intercalated water in multilayered graphene oxide. ACS Nano 2010;4(10):5861–8.
[42] Wang YY, Ni ZH, Shen ZX, Wang HM, Wu YH. Interference enhancement of Raman signal of graphene. Appl Phys Lett 2008;92(4).
[43] Jung I, Vaupel M, Pelton M, Piner R, Dikin DA, Stankovich S, et al. Characterization of thermally reduced graphene oxide by imaging ellipsometry. J Phys Chem C 2008;112(23):8499–506.